AIAA 2000-0093

Mixing Enhancement Using Axial Flow

Dimitri Papamoschou

Dept. of Mechanical & Aerospace Engineering
University of California at Irvine
Irvine, CA

38th Aerospace Sciences Meeting & Exhibit
10-13 January 2000 / Reno, NV

AIAA-2000-0093

Mixing Enhancement Using Axial Flow *

Dimitri Papamoschou †
Department of Mechanical and Aerospace Engineering
University of California, Irvine
Irvine, CA 92697-3975

Flow exiting a convergent-divergent nozzle operated at off-design conditions exhibits a strong instability that causes mixing enhancement in the flow itself and can destabilize an adjacent flow. The latter property enables mixing enhancement of an arbitrary jet via parallel injection of a secondary gas flow. Furthermore, flow in existing coaxial arrangements, wherein the outer stream is gaseous and operates within a certain pressure range, can be destabilized by minor geometric changes. The paper describes the discovery of this phenomenon, presents an overview of experiments at U.C. Irvine, and discusses the possible connection to supersonic nozzle flow separation. A roadmap for better understanding and utilization of the instability mechanism is proposed.

I. Introduction

A strange occurrence of mixing enhancement was observed in coaxial jet noise experiments conducted at UCI. The jets were composed of a round supersonic stream (primary flow) surrounded by an annular gas stream of variable velocity and density (secondary flow or coflow). With the conditions of the primary flow fixed and with increasing velocity of the secondary flow from low subsonic to sonic to supersonic, the following trends were observed. First, the spreading rate of the primary stream declined, as expected from the reduced velocity difference across the shear layer. As the secondary flow reached near-sonic conditions (ideally-expanded Mach number in the approximate range of 0.8 to 1.2), the spreading rate was significantly enhanced, an unexpected deviation. An example of this deviation is shown in Fig. 1, where an annular coflow enhances mixing of a supersonic jet surrounded by the coflow. With increasing, supersonic velocity of the secondary flow, the spreading rate decreased from the enhanced state and eventually returned to normal values. The puzzling departure near the sonic point triggered a systematic investigation of this phenomenon at UCI, starting in 1996, and NASA Glenn Research Center two years later [1]. Before proceeding with a desription of the UCI experiments, it is useful to review the significance of mixing enhancement and the state of the art in mixing enhancement methods.

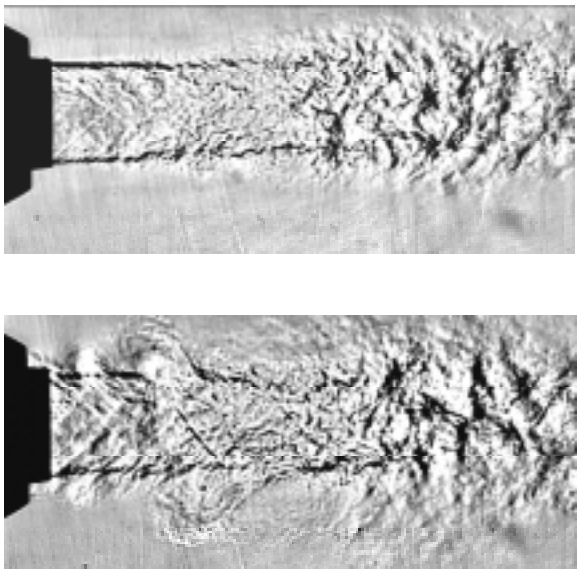

Fig.1 Effect of an annular, unstable coflow on a Mach 1.5 jet. (a) Single jet; (b) coaxial jet.

*U.S. Patent Pending
†Professor, member AIAA

The vast majority of our energy and propulsive power comes from burning fuels. Fuel efficiency and reduction of toxic emissions are governed by the completeness of the mixing process between fuel and oxidizer [2]. Ideally, fuel and oxidizer mix at the molecular level in the desired proportion before reacting. Incomplete or non-uniform mixing leads to unburned reactants with resulting loss in efficiency and production of pollutants such as soot particles and nitric oxides [3]. The ideal case is extremely difficult to achieve in practice. A major constraint is the finiteness of space and/or time available for mixing. In the combustor of a jet engine, for instance, fuel and air must mix at high velocity within a very short length. In reciprocating engines, fuel must be introduced and mixed in the piston cylinder within a few milliseconds. These challenges apply to both gaseous and liquid fuels, although liquid fuels are more difficult to mix because a liquid stream must go through several stages before complete reaction can occur: breakup, atomization, vaporization, and molecular mixing with the oxidizer [4]. Another difficulty is the simultaneous achievement of mixing enhancement and sufficient penetration into the combustion zone. Examples where penetration is critical are injection into the cylinder of a diesel engine and transverse injection into a crossflow [5]. Conventional devices such as lobe mixers [6], swirlers [7], and airblast atomizers [8] achieve mixing with an attendant reduction in the axial momentum of the flow, which reduces penetration. A further consideration is simplicity and compactness of the nozzles. Good mixing does not guarantee operational success if the mixer is too complicated, too large, or too heavy.

In aircraft exhaust systems, mixing enhancement has been motivated by the need to suppress noise and thermal emissions. Mechanical schemes have included lobe mixers [9, 10]; vortex generators, mainly in the form of tabs [11, 12]; and nozzle cutouts [13]. Major drawbacks are thrust penalty (with notable exception of the cutouts, which inflict minimal thrust loss but require imperfect expansion of the jet), weight penalty, and complexity of the engine exhaust. Thrust losses escalate with increasing jet Mach number and can easily reach the order of 10% in supersonic jets [14, 15]. Complexity of the engine exhaust means increased manufacturing and maintenance costs. In the general area of high-speed shear layers, efforts to increase mixing have included cavity actuators [17], shock impingement [18], trailing edge modifications [19], and sub-boundary layer disturbances [20]. The obvious tradeoff is mixing versus total pressure loss. The least-intrusive methods increase the growth rate modestly, while the forceful ones increase mixing at the expense of aerodynamic performance. Efficient mixing enhancement at high speeds remains one of the toughest challenges of fluid mechanics.

The desire to find alternatives to mechanical mixers has sparked research on fluidic control of jets. The counter-current shear layer of Strykowksi et al. [21] demonstrated a substantial increase in the mixing rate compared to the classical flow. Application of a counterflow on an engine exhaust or fuel injector has the obvious drawback of momentum loss, although other properties of counterflow have been ingeniously exploited towards thrust vectoring [22]. Significant effort has also been directed to pulsed-jet control, where unsteady transverse jets installed at the jet exit destabilize the plume [23, 24]. While impressive increases in the jet entrainment rate have been recorded, practical implementation presents several challenges, including impact on system performance and loss of axial momentum. Synthetic jets [25] are showing substantial promise in controlling subsonic gas flows; their efficacy in supersonic environments has not yet been demonstrated.

The mixing enhancement method described in this paper is different from the above techniques in two essential aspects: first, it does not use mechanical devices to directly disturb the flow; second, it uses parallel injection to destabilize the flow, in contrast with the counter-flow and transverse-flow fluidic schemes mentioned above.

II. Mixing Enhancement Using Axial Flow

The UCI effort has spanned three years and hundreds of experiments. It is not possible or instructive for one paper to cover all the cases examined. This section presents selected experiments that help illuminate and quantify the mixing enhancement phenomenon. Table 1 lists the flow conditions corresponding to the key figures presented.

A. Axisymmetric Nozzle Shapes

Following the initial observation of mixing enhancement described in the Introduction, attention was focused on the shape of the annular nozzles supplying the secondary stream. Figures 2(a) and (c) present the specific geometry of two nozzles for which mixing enhancement was first observed. Both nozzles featured a small increase in cross-sectional area near the exit, thus forming a convergent-divergent annular duct. The nominal (coplanar) exit-to-minimum area ratios were

sion.

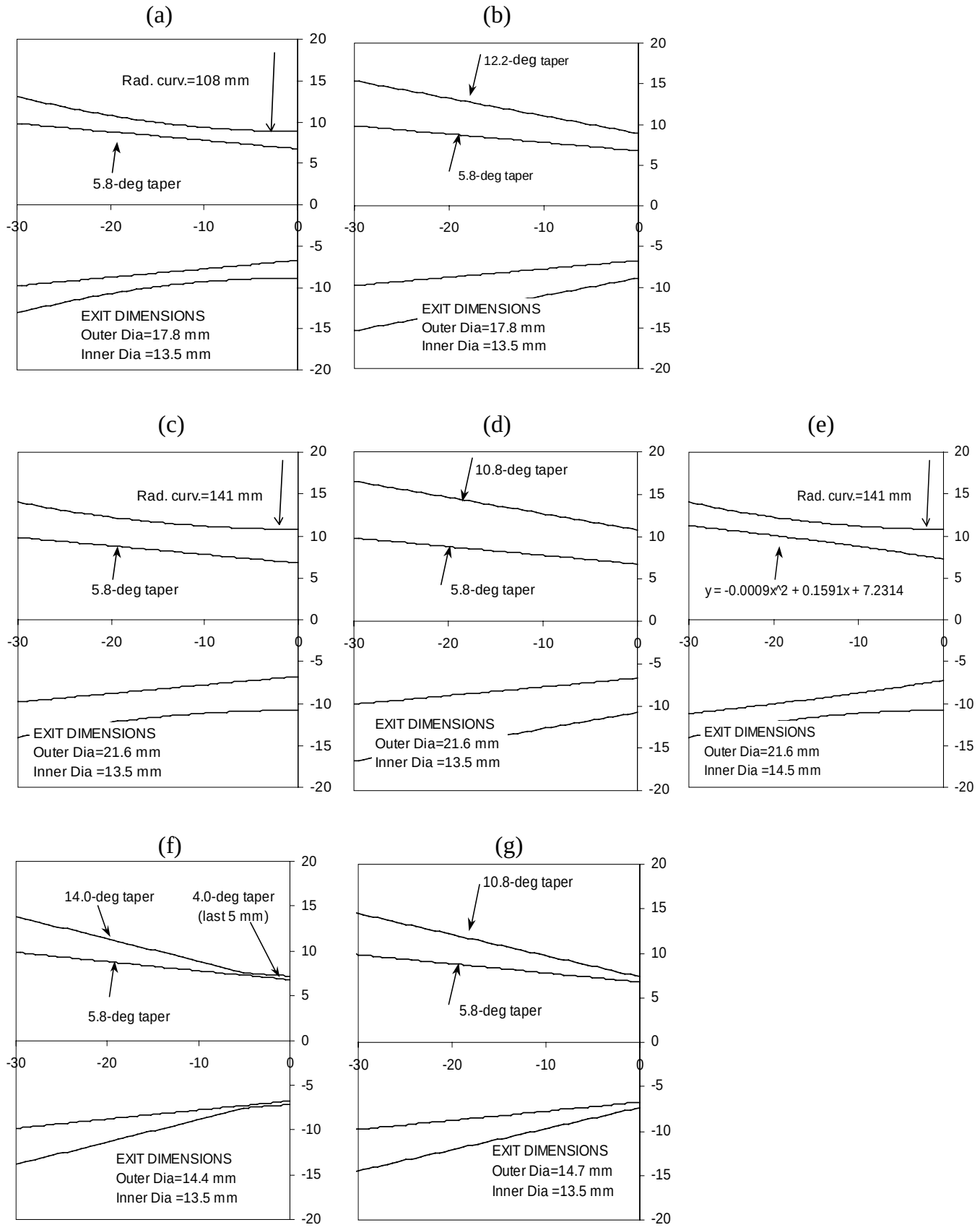

Fig.2 Radial coordinates of axisymmetric coaxial nozzles used in the UCI tests. Dimensions are in millimeters. All arrangements except 2(e) featured the same inner nozzle whose inner duct, not shown, was designed for Mach 1.5 flow. First column: convergent-divergent coflow nozzles; second column: counterpart convergent nozzles; third column: special arrangement using the outer nozzle of 2(c) but a different inner nozzle with constant-area inner duct.

Table 1 Flow Conditions

FIG	NOZZLE	NPR_1	M_1	U_1	Re_1	NPR_2	M_2	U_2	Re_2	$A_e/A_{\min}$	$\dot{m}_2/\dot{m}_1$	F_2/F_1
5a, 6a	Mach 1.5	3.67	1.50	430	5.5E5	-	-	-	-	-	-	-
5c, 6b	Fig. 2a	3.67	1.50	430	5.5E5	1.75	0.93	290	4.0E4	1.25	0.42	0.29
5b	Fig. 2b	3.67	1.50	430	5.5E5	1.75	0.93	290	4.0E4	conv.	0.42	0.29
8	Fig. 2a	3.67	1.50	430	5.5E5	var.	var.	var.	var.	1.25	-	-
9a	Fig. 2b	-	-	-	-	1.75	0.90	410	2.8E4	conv.	-	-
9b	Fig. 2a	-	-	-	-	1.75	0.90	410	2.8E4	1.25	-	-
10	Fig. 2b	-	-	-	-	1.68	0.89	280	3.8E4	conv.	-	-
	Fig. 2a	-	-	-	-	1.68	0.89	280	3.8E4	1.25	-	-
11	Fig. 2b	-	-	-	-	var.	var.	var.	var.	conv.	-	-
	Fig. 2a	-	-	-	-	var.	var.	var.	var.	1.25	-	-
12a	Fig. 2d	-	-	-	-	1.78	0.92	420	6.2E4	conv.	-	-
12b	Fig. 2c	-	-	-	-	1.78	0.92	420	6.2E4	1.11	-	-
13a	Mach 1.0	3.40	1.44	420	5.5E5	-	-	-	-	-	-	-
13b	Fig. 2e	3.40	1.44	420	5.5E5	1.84	0.97	310	5.7E4	1.50	0.47	0.36
15a	Fig. 2b	1.70	0.90	465	1.8E5	1.71	0.91	290	4.6E4	conv.	1.35	0.86
15b	Fig. 2a	1.70	0.90	465	1.8E5	1.71	0.91	290	4.0E4	1.25	1.20	0.75
15c	Fig. 2c	1.70	0.90	465	1.8E5	1.71	0.91	290	3.6E4	1.35	1.20	0.75
16	Fig. 2b	1.75	0.90	320	3.0E5	1.61	0.85	270	3.6E4	conv.	0.73	0.70
16	Fig. 2a	1.75	0.90	320	3.0E5	1.61	0.85	270	3.6E4	1.25	0.73	0.70
17a	Fig. 2d	1.67	0.86	435	1.7E5	1.77	0.94	300	8.7E4	conv.	3.28	2.26
17b	Fig. 2c	1.67	0.86	435	1.7E5	1.77	0.94	300	8.7E4	1.11	3.28	2.26
18a	Fig. 2g	3.67	1.50	430	5.5E5	1.80	0.96	300	1.1E4	conv.	0.13	0.09
18b	Fig. 2f	3.67	1.50	430	5.5E5	1.80	0.96	300	1.1E4	1.3	0.09	0.07
20a	Fig. 19	3.67	1.50	430	6.0E5	-	-	-	-	-	-	-
20b	Fig. 19	3.67	1.50	430	6.0E5	2.00	1.05	320	9.6E4	conv.	0.33	0.25
20c	Fig. 19	3.67	1.50	430	6.0E5	2.00	1.05	320	9.6E4	1.3	0.33	0.25
22a	Fig. 2a	3.67	1.50	430	5.5E5	1.64	0.87	280	3.7E4	1.25	0.40	0.26
22b	Fig. 2a	3.67	1.50	430	5.5E5	1.51	0.79	260	3.3E4	1.25	0.38	0.23

NPR=nozzle pressure ratio

U in m/s

M is ideally-expanded Mach number

Re is based on actual (hydraulic) diameter of primary round (rectangular) jet and on minimum height and associated conditions for coflow.

F is thrust based on ideal expansion

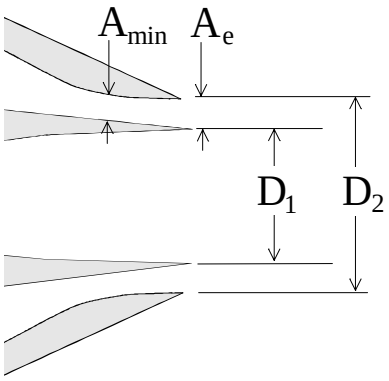

Fig.3 Generic shape of mixing-enhancement nozzle. Outer (coflow) duct is convergent-divergent. The coflow pressure ratio is such as to cause sonic velocity at the minimum area of the duct and an adverse pressure gradient near the exit of the duct. The properties of the inner steam are irrelevant to the mechanism of the instability.

1.25 for the smaller nozzle and 1.11 for the larger nozzle. The increase in exit area was inadvertent; ideally, the annular duct should have been parallel at the exit. It was an oversight of the author who did not incorporate the small taper of the outer wall of the inner nozzle in his design of the inner contour of the outer nozzles. The small area increase of the nozzles – particularly of the larger nozzle which was heavily utilized in the initial noise tests – seemed insignificant at the time. Indeed, it would have been so if the nozzles were operated at low-to-moderate subsonic Mach numbers. For high-subsonic or sonic flow, however, the nozzles produced an instability which was evident in schlieren pictures and in centerline Mach number measurements. Having realized that the divergence created such a profound effect, new nozzles of conical convergent shape were built for the noise research. The radial coordinates of the annular nozzles covered in this paper are summarized in Fig. 2. The first column describes the convergent-divergent nozzles and the second column their counterpart convergent nozzles. The inner surface of the annular passage (the outer wall of a Mach 1.5 nozzle) was identical for all the nozzles depicted in the first two columns. The third column, Fig. 2(e), depicts a special arrangement that used a different inner nozzle. Installation of the nozzles allowed certain flexibility in the relative axial placement of the inner and outer nozzles. Given the taper of the inner surface, this allowed some variation of the nozzle exit area and, in the case of the convergent-divergent nozzles, the exit-to-minimum area ratio. The convergent nozzles were typically recessed relative to their convergent-divergent counterparts to produce the same mass flow rate when subjected to the same nozzle pressure ratio.

As will be shown next, the convergent nozzles never produced mixing enhancement at any pressure ratio.

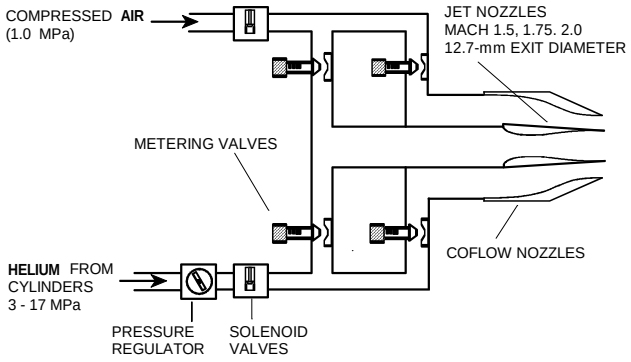

Fig.4 Coaxial jet facility.

It was clear, therefore, that mixing enhancement was connected with the operation of a convergent-divergent nozzle at pressure ratios well below the design (fully-expanded) value. The generic nozzle configuration is illustrated in Fig. 3. A critical parameter is the ratio of exit area to minimum area, $A_e/A_{\min}$, of the coflow nozzle. The properties of the primary stream are irrelevant to the instability mechanism, therefore *the conditions of the primary stream can be arbitrary.* This implementation is called Mixing Enhancement via Secondary Parallel Injection (MESPI) and can be applied to subsonic, supersonic, and even liquid streams, thus has broad potential for practical applications.

B. Axisymmetric Jets

Axisymmetric tests were conducted in the coaxial jet facility depicted in Fig. 4. The inner nozzles of 12.7-mm exit diameter were designed by the method of characteristics for Mach numbers $M_1 = 1.5$, 1.75, and 2.00. Occasionally, the Mach 1.5 nozzle was operated at low pressure ratio to produce subsonic outflow. This paper covers only the Mach 1.5 and subsonic tests. A variety of outer nozzles, some shown in Fig. 2, formed the annular passage for the coflow. Precisely-metered mixtures of helium and air were supplied to the nozzles, which exhausted into ambient, still air. Helium-air mixtures duplicate well the density, velocity, and speed of sound of a heated jet. Pressure transducers recorded the total pressures in the jet and coflow streams, and the pressure of a pitot probe translated along the centerline of the jet. In some cases, a microphone (Bruel & Kjaer, Model 4138) recorded the noise emitted by the jet. A schlieren system with 20-nanosecond spark source (Xenon, Model N787) and 150-mm beam diameter was used for instantaneous flow visualization. Schlieren photography was occasionally complemented by pulsed planar laser induced fluorescence, using gaseous acetone as the tracer molecule and the ultraviolet output of an Nd:Yag laser (Continuum, Surelite II) for excitation. Further details

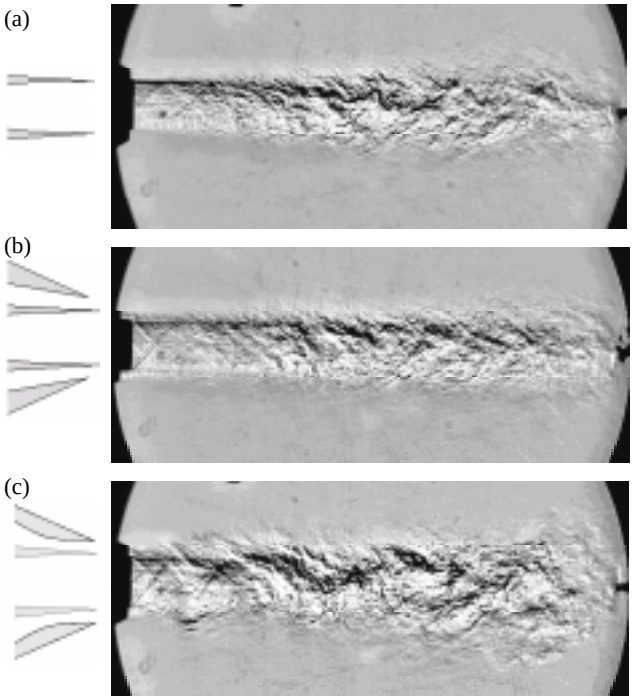

Fig.5 Schlieren images of Mach-1.5, 450-m/s air jets: (a) no coflow; (b) coflow issuing from a convergent annular duct; (c) coflow issuing from a convergent-divergent annular duct with A_e/A_{min}=1.25. The combined flows have 40% larger mass flow rate and 30% higher thrust than the single jet.

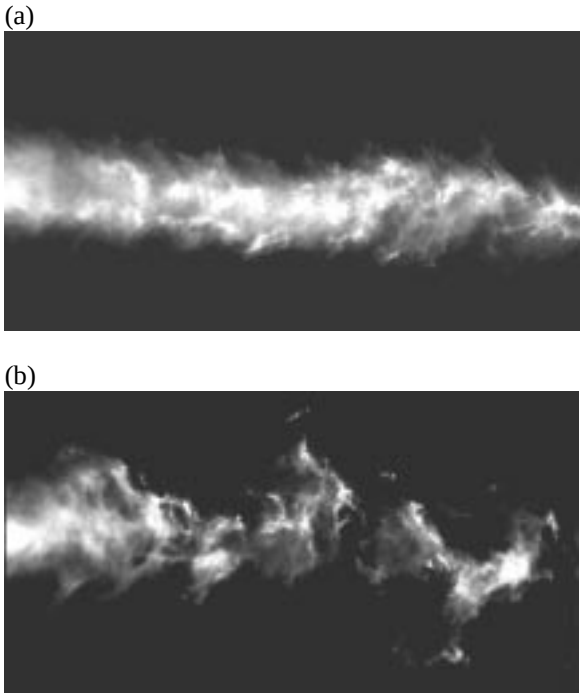

Fig.6 PLIF images of the flows of (a) Fig. 5(a); and (b) Fig. 5(c). Field of view is six jet diameters wide and starts six jet diameters downstream of the nozzle exit.

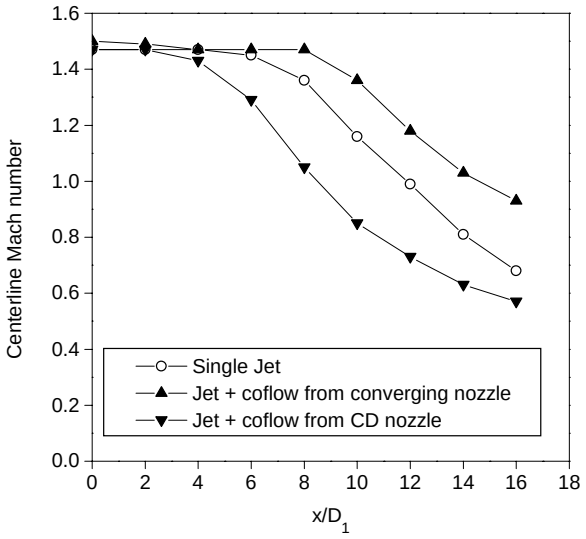

Fig.7 Centerline Mach number distributions for cases of Fig. 5.

on the facility and diagnostics can be found in [27].

Figure 5 presents schlieren images of three cases, all involving the same primary air jet at Mach 1.5. Depicted are the single jet in Fig. 5(a); the jet surrounded by a coflow from a convergent nozzle in Fig. 5(b); and the jet surrounded by a coflow from a convergent-divergent nozzle in Fig. 5(c). In the latter two cases, the coflow was supplied at a nozzle pressure ratio NPR=1.75 and the mass flow rates were equal. Application of the coflow from a convergent nozzle, Fig. 5(b), stabilized the jet as expected from the reduced velocity difference across the jet's shear layer. The coflow from the convergent-divergent nozzle, however, had the opposite effect and destabilized the jet. Further evidence of the instability induced by the coflow is offered in the planar laser induced fluorescence (PLIF) images of Fig. 6, corresponding to the flows of Figs. 5(a) and (c).

A quantitative measure of mixing enhancement is the decay of centerline Mach number with axial distance. The faster the decay, the stronger the mixing of the primary flow with the ambient fluid. Figure 7 depicts centerline Mach number distributions for the cases of Fig. 5. The potential core of the single jet ends at roughly $x/D_1 = 6$. Application of the coflow from the convergent nozzle, lengthened the core to about $x/D_1 = 8$, while the coflow from the convergent-divergent nozzle shortened the core to about $x/D_1 = 4$. Strictly speaking, to make quantitative assessment of mixing enhancement one should compare flows of equal mass flow rate and equal thrust. This is possible here by comparing the axial Mach number distributions for the two coaxial flows, which have equal mass flow rate and roughly (within a few percent) equal thrust. The divergence of the coflow nozzle resulted in a 50% reduction

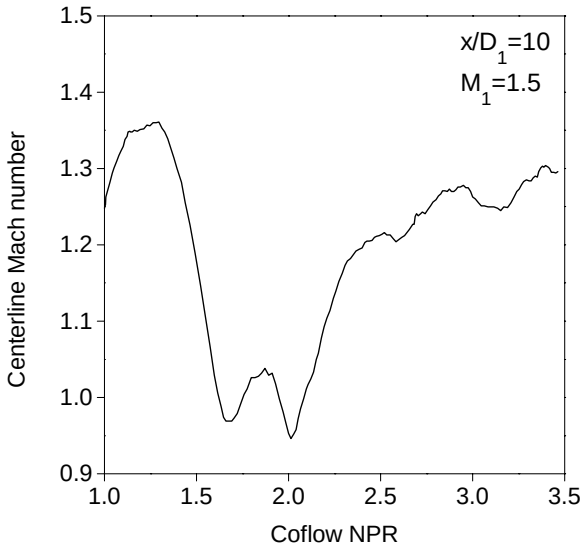

Fig.8 Centerline Mach number at $x/D_1 = 10$ versus coflow NPR for the arrangement of Fig. 5(c). Inner flow is a Mach 1.5 air jet.

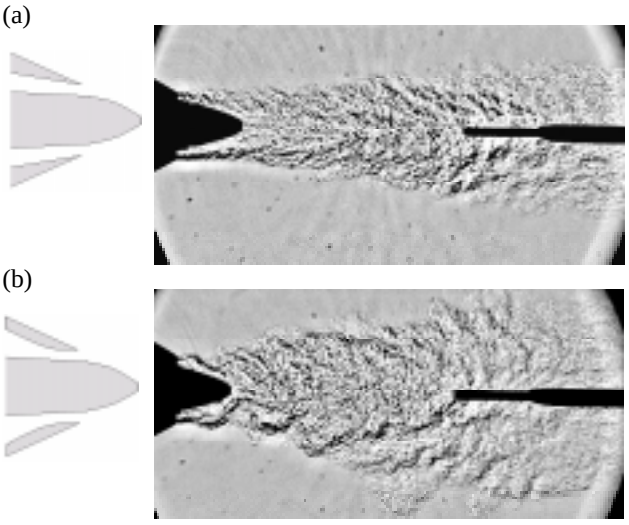

Fig.9 Schlieren images of annular jets composed of a helium-air mixture. Ideally-expanded Mach number is 0.9 and velocity is 410 m/s for both jets. (a) Annular nozzle is convergent; (b) annular nozzle is convergent-divergent with $A_e/A_{\text{min}} = 1.25$. The two jets had the same mass flow rate. Centerline Mach number at $x/D_2 = 4.2$ dropped from 0.77 in (a) to 0.48 in (b).

in the length of the potential core and a 40% reduction in the centerline Mach number at $x/D_1 = 10$. The unequal comparison between the single jet of Fig. 5(a) and the combined flow of Fig. 5(c) (which has 42% more mass flow rate and 29% higher thrust than the single jet) shows that the coaxial flow mixed faster with the surrounding air than did the single jet. In other words, addition of the coflow resulted here in net mixing enhancement. Obviously, if the coflow became very large, this would not be the case. Net mixing enhancement between the inner jet and the ambient is expected to occur if the mass flow rate of the coflow is a fraction of that of the jet. Figure 8 presents the variation of centerline Mach number at $x/D_1 = 10$ versus coflow nozzle pressure ratio for the arrangement of Fig. 5(c). As NPR increased from 1.0, the centerline Mach number increased, signifying mixing suppression. At around NPR=1.4, the trend reversed and the centerline Mach number declined rapidly (mixing enhancement), staying at low levels until about NPR=2.5. Above this NPR, the centerline Mach number rose to values that seem consistent with the lack of mixing enhancement. Figure 8 thus gives an idea of the coflow nozzle pressure ratio for which mixing enhancement occurs when one uses this particular coflow nozzle.

We now turn our attention to cases where only the coflow was turned on. The inner nozzle normally supplying the jet was terminated with a streamlined plug; the outer nozzles were those described in Figs. 2(a) and (b). In essence, the coflow assumed the role of the jet. Figure 9 compares schlieren images of two such jets, one issuing from an annular convergent nozzle and the other from an annular convergent-divergent nozzle

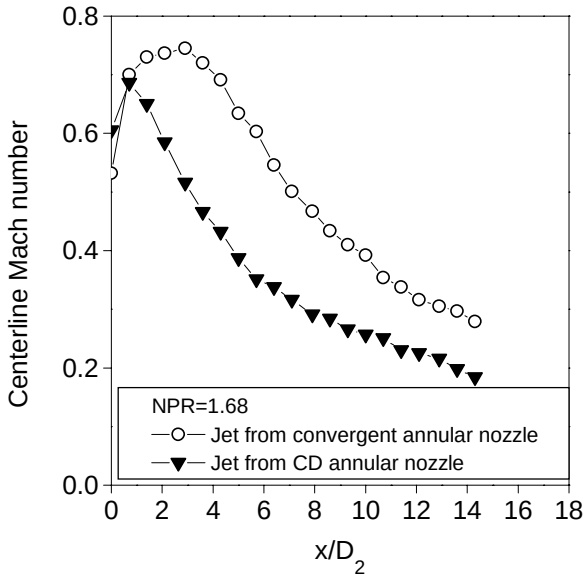

Fig.10 Centerline Mach number distributions for annular air jets issuing from a convergent nozzle and from a convergent-divergent nozzle. NPR= 1.68 and the mass flow rate was equal for both jets.

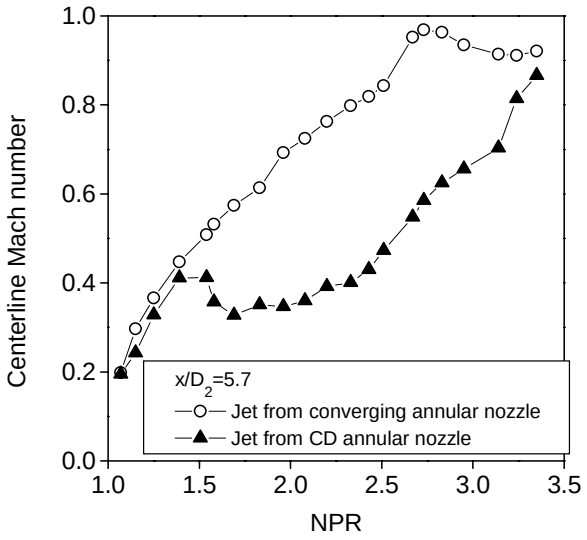

Fig.11 Centerline Mach number at $x/D_2 = 5.7$ versus NPR for annular air jets issuing from a convergent nozzle and from a convergent-divergent nozzle. At each NPR, the two jets had the same mass flow rate.

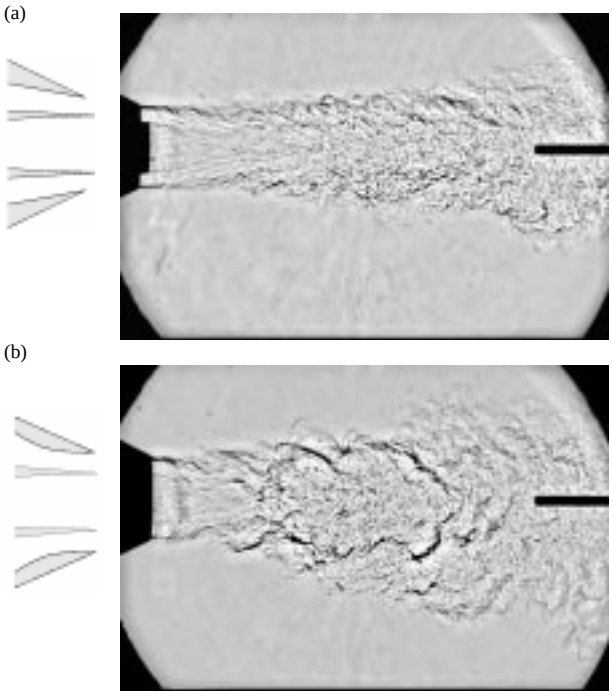

Fig.12 Schlieren images of large annular jets composed of a helium-air mixture. Ideally-expanded Mach number was 0.9 and velocity was 420 m/s for both jets. (a) Annular nozzle is convergent; (b) annular nozzle is convergent-divergent, with $A_e/A_{\min} = 1.11$. The two jets had the same mass flow rate. Centerline Mach numbr at $x/D_2 = 4.7$ dropped from 0.77 in (a) to 0.63 in (b).

with $A_e/A_{\min} = 1.25$. Both nozzles were supplied by a helium-air mixture at nozzle pressure ratio NPR=1.75 and produced the same mass flow rate. The jet from the convergent-divergent nozzle spread roughly three times faster than the jet from the convergent nozzle. Figure 10 shows the axial variation of centerline Mach number $M_{\mathrm{C/L}}$ for cases similar to those of Fig. 9 but with air replacing the helium-air mixture. The instability associated with the convergent-divergent nozzle caused a marked decrease in $M_{\mathrm{C/L}}$ starting at a short distance from the nozzle exit. The reduction reached 40% at $x/D_2 = 5$. Figure 11 shows the variation of $M_{\mathrm{C/L}}$ with NPR at fixed axial position $x/D_2 = 5.7$ for the two configurations of Fig. 9, with air in the coflow. This plot is analogous to that of Fig. 8 for the supersonic jet. As NPR increased from 1.0, $M_{\mathrm{C/L}}$ rose identically for both nozzles until NPR=1.36 was reached. Immediately past this value, $M_{\mathrm{C/L}}$ for the convergent-divergent nozzle dropped with increasing NPR, while $M_{\mathrm{C/L}}$ for the convergent nozzle continued rising. Thus, NPR=1.36 marks the start of the mixing enhancement for this particular nozzle. At NPR$\approx$1.5, $M_{\mathrm{C/L}}$ for the convergent-divergent nozzle started rising again but at a value about 40% below that of the convergent nozzle. The difference between the two nozzles closed at around NPR=3.0, which suggests the end of mixing enhancement. The best mixing enhancement, in terms of percent drop in $M_{\mathrm{C/L}}$, occurred for $1.5 <$ NPR < 2.5. Figure 12 presents schlieren images analogous to those of Fig. 9 but with a larger annulus, utilizing the nozzles of Figs. 2(c) and (d). No plug was installed on the inner nozzle in this case. The trends are similar to those in Fig. 9, even though the convergent-divergent nozzle had a smaller area ratio $A_e/A_{\min} = 1.11$.

To test the robustness of the mixing enhancement phenomenon, the finely-machined aluminum inner nozzle was replaced by a rather crude plastic nozzle. It was fabricated from a short PVC pipe by grinding one of its ends into a taper. No particular contour was imposed; the final shape, shown in Fig. 2(e), was *ad-hoc*. The inner duct was parallel, giving sonic exit when subjected to a pressure ratio above 1.89. Figure 13 shows schlieren images of a sonic, underexpanded jet without and with coflow at NPR=1.84. Mixing enhancement was very strong, which could be attributed to the larger expansion ratio of this coflow nozzle ($A_e/A_{\min} = 1.5$). The plastic nozzle was thereafter instrumented with pressure taps to record the pressure distribution on its surface. It was possible to drill only a small number of taps, so the spatial resolution was crude. The taps were connected to thin copper tubes running through the inner passage of the nozzle and protruding a long distance from the nozzle exit, at which point they were connected to pressure transducers via nylon tubing. This arrangement precluded the operation of the in-

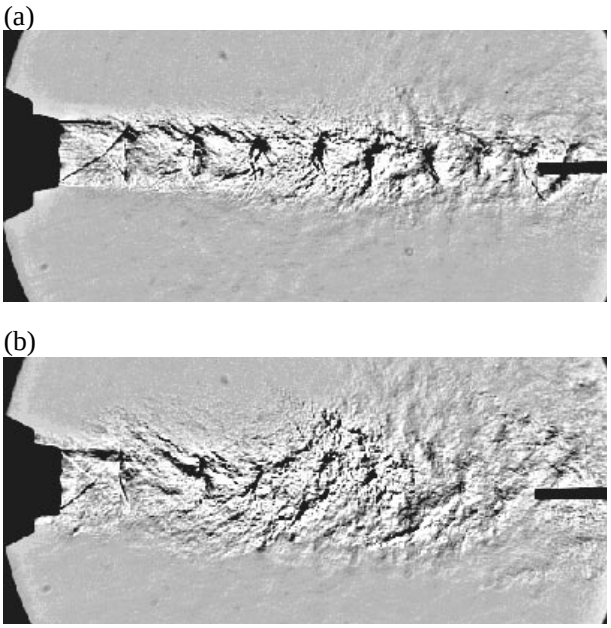

Fig.13 Schlieren images of an underexpanded sonic jet supplied at NPR=3.2 (a) alone and (b) surrounded by coflow from convergent-divergent nozzle with NPR=1.84. Centerline Mach number at $x/D_1 = 8$ dropped from 1.27 in (a) to 0.87 in (b).

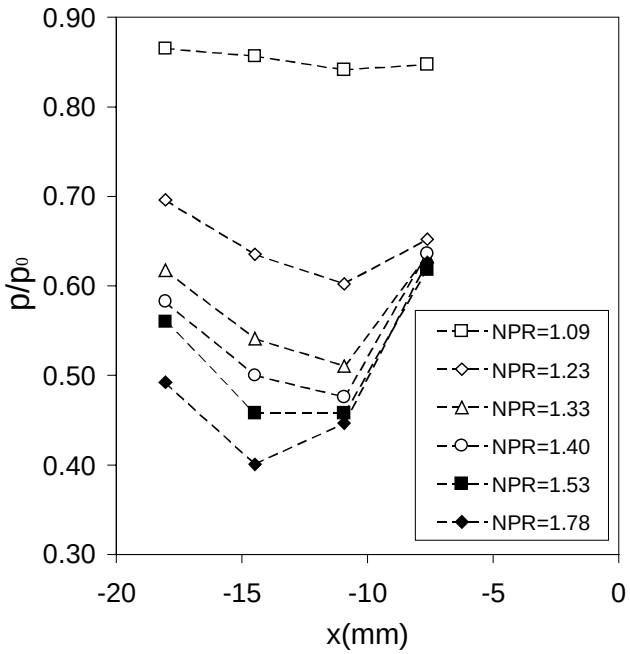

Fig.14 Static pressure distribution on the outer wall of the inner nozzle of Fig. 2(e). Axial distance is measured from lip of inner nozzle. Annular nozzle supplying coflow terminated at $x = -5$ mm. The data for NPR=1.78 correspond closely to the flow shown in Fig. 13(b).

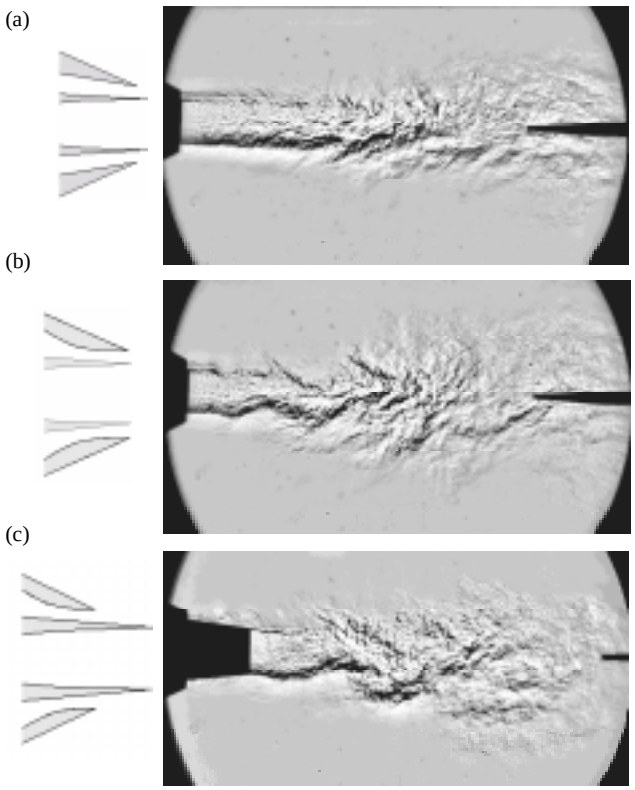

Fig.15 Schlieren images of Mach-0.9, 465-m/s helium-air jets: (a) coflow issuing from a convergent annular duct; (b) coflow issuing from a convergent-divergent annular duct with A_e/A_{min}=1.25. (c) coflow issuing from a recessed convergent-divergent annular duct with A_e/A_{min}=1.35. The mass flow rates were approximately equal in all cases. Centerline Mach number at x/D_1=8 dropped from 0.73 in (a) to 0.58 in (b) to 0.52 in (c).

ner stream. Since the instability depends only on the coflow conditions, absence of the inner stream should not impact the relevance of the results. Figure 14 plots the static-to-total pressure ratio, p/p_0, versus axial distance for a variety of NPRs. The pressure distributions associated with mixing enhancement correspond to acceleration of the flow to sonic velocity followed by an adverse pressure gradient near the nozzle exit. It will be shown later that this is consistent with flow separation inside the nozzle.

We now examine coaxial cases with a subsonic primary jet. In Fig. 15, the primary flow consisted of a helium-air mixture at Mach 0.9 and velocity of 465 m/s. The coflow was air, supplied at NPR=1.71. In Fig. 15(a), the coflow was supplied by the converging nozzle of Fig. 2(b); the low spreading rate of the primary jet is evident. Changing the coflow nozzle to the convergent-divergent one of Fig. 2(a), the primary jet became very unstable as shown in Fig. 15(b). In Fig. 15(c), the coflow nozzle was recessed 20 mm upstream of the jet exit. To maintain the same mass flow rate as in the

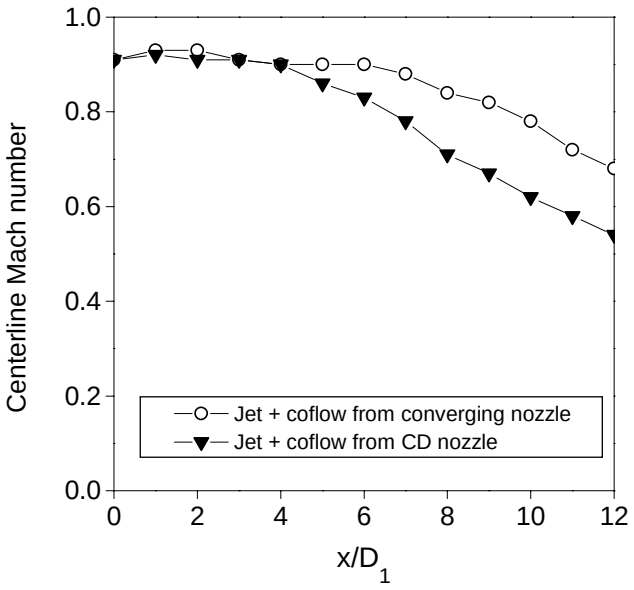

Fig.16 Centerline Mach number distributions for Mach 0.9 air jets with coflow at NPR=1.61 issuing from convergent and convergent-divergent annular nozzles. The setup is the same as in Figs. 15 (a) and (b), except that the jet is composed of air.

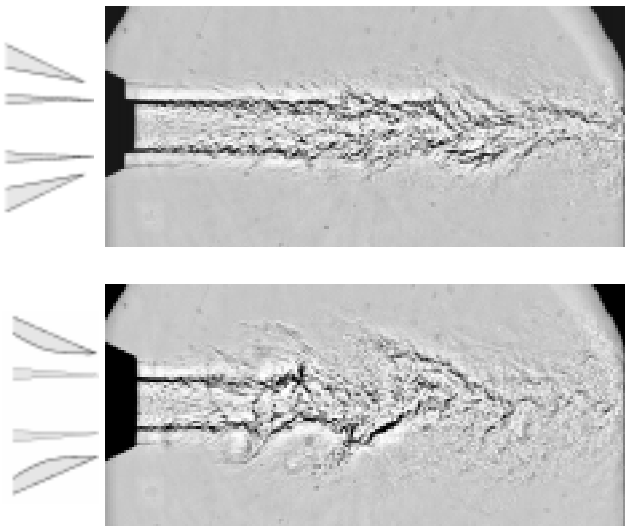

Fig.17 Schlieren images of Mach-0.9, 450-m/s air jets with large coflow annulus: (a) coflow duct is convergent; (b) coflow duct is convergent-divergent with A_e/A_{min}=1.1. Both flows have equal mass flow rate. Centerline Mach number at x/D_1=10 dropped from 0.76 in (a) to 0.63 in (b).

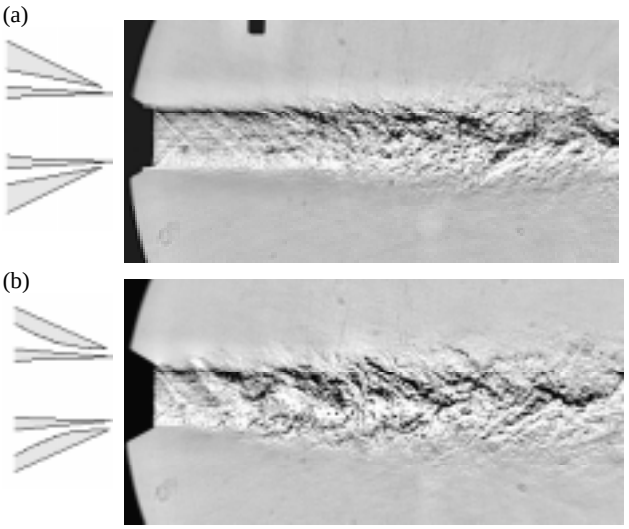

Fig.18 Schlieren images of Mach-1.5, 450-m/s air jets with very thin coflow annulus: (a) coflow duct is convergent; (b) coflow duct is convergent-divergent with A_e/A_{min}=1.3. Both flows have equal mass flow rate. Centerline Mach number at x/D_1=10 dropped from 1.34 in (a) to 1.04 in (b)

previous two cases, the larger nozzle of Fig. 2(c) was used. The jet was as unstable as with the coplanar nozzle, indicating that the instability is not very sensitive on the relative axial placement of the jet and coflow nozzles. Figure 16 presents centerline Mach number distribution for a setup similar to that of Figs. 15(a) and (b) but with air in the primary jet. The mixing enhancement of the coflow from the convergent-divergent nozzle is again evident. These flows are similar to those tested at NASA Glenn Research Center in a larger facility [1]. Figure 17 shows the effect of a large coflow on the growth rate of a Mach 0.9, 450-m/s jet. The $A_e/A_{\text{min}} = 1.11$ divergence of the coflow nozzle had a pronounced effect on mixing. The flows of Fig. 17 are representative of the exhaust of a turbofan engine with bypass ratio around 3. These experiments suggest that a subtle redesign of the fan nozzle can lead to the kind of mixing enhancement seen in Fig. 17. For this type of engine, mixing between the jet and fan (coflow) could be as important as mixing between the jet and ambient flows (for reducing infrared signature, for example.) In an arrangement where the jet and coflow are supplied at the same total pressure, the centerline Mach number distribution does not describe the mixing rate between jet and coflow. Other means of quantifying mixing, such as the diffusion of a passive scalar, would be necessary.

Figure 18 compares supersonic jets surrounded by very thin coflows issuing from the nozzles of Figs. 2(f) and (g). Despite the very low flow rate of the coflow stream (9% of the primary jet), the convergent-divergent nozzle induces noticeable mixing enhancement. The piece-

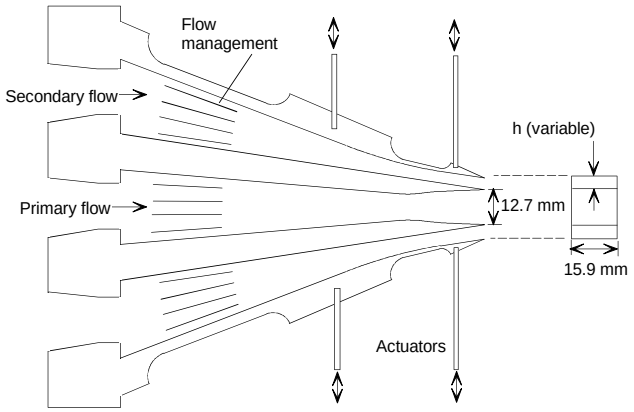

Fig.19 Rectangular dual-stream jet apparatus with secondary flow of variable exit height and adjustable nozzle shape. Upstream actuators controlld the exit height; downstream actuators controlled the nozzle shape.

wise conical design of this nozzle, with a cornered expansion, is far from ideal. A contoured nozzle may have given better performance.

C. Rectangular Jets

Rectangular jet experiments were conducted in the dual-stream apparatus depicted in Fig. 19. The primary stream was supplied by an inner nozzle, designed by the method of characteristics for Mach number 1.5. Its exit dimensions were 12.7 mm in height and 15.9 mm in width. The secondary stream was supplied by two outer nozzles incorporating flexible walls for adjustment of their exit height and for changing their contour. The width of the secondary stream was 15.8 mm, same as that of the primary stream. The apparatus was connected to the same gas supply system that fed the axisymmetric jets (Fig. 4). The diagnostics were the same as those used in the axisymmetric jets. The apparatus was originally designed to supply a dual stream within the confines of an ejector, hence its low aspect ratio of 1.2. It is not an ideal facility for studying free-jet mixing enhancement because only the top and bottom surfaces of the jet are surrounded by the coflow – the sides are not. As such, this jet displays certain idiosyncracies which would not have occurred if it were uniformly surrounded by a coflow. However, the ability to change the nozzle contour (from convergent to convergent-divergent) allowed preliminary experiments to determine if mixing enhancement also occurs in rectangular nozzles.

Figure 20 presents schlieren images of three rectangular cases, all involving the same primary air jet at Mach 1.5. Depicted are the single jet in Fig. 20(a); the jet surrounded by a coflow from a convergent nozzle in Fig. 20(b); and the jet surrounded by a coflow from a

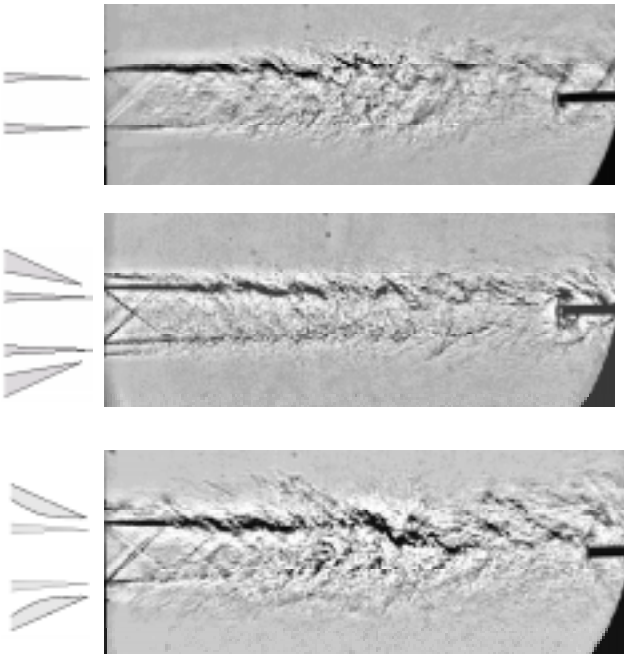

Fig.20 Schlieren images of rectangular Mach-1.5, 450-m/s air jets: (a) no coflow; (b) coflow issuing from a convergent annular duct; (c) coflow issuing from a convergent-divergent annular duct with A_e/A_{min}=1.3. The combined flows have 33 % larger mass flow rate and 25 % higher thrust than the single jet.

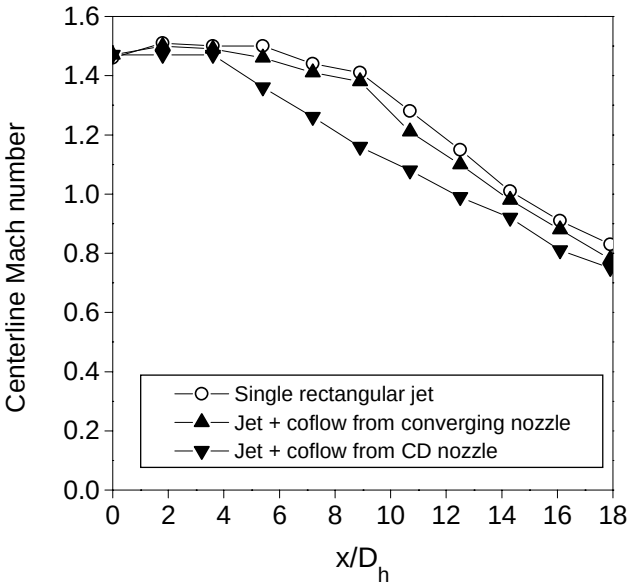

Fig.21 Centerline Mach number distributions for the cases of Fig. 20.

convergent-divergent nozzle in Fig. 20(c). In the latter two cases, the coflow was supplied at a nozzle pressure ratio NPR=2.0 and the mass flow rates were equal. The trends are the same as those in the axisymmetric cases. The coflow from a convergent nozzle stabilizes the jet while that from the convergent-divergent nozzle destabilizes it. The jet of Fig. 20(c) is seen to have a higher growth rate than the single jet of Fig. 20(a). The centerline Mach number distributions for these cases are shown in Fig. 21. Interestingly, the curves for the single jet and for the jet plus convergent coflow practically overlap, although one would have expected the combined flow to mix slower. It is believed that the coflow, whose exit direction is slighly inclined towards the jet axis, squeezed the jet in the transverse direction, leading to increased spreading of the jet in the lateral direction (recall that the jet is unbounded in that direction). Even though transverse spreading was suppressed, the increase of the lateral spreading led to an overall mixing rate comparable to that of the single jet. The coflow from the convergent-divergent nozzle had a pronounced effect on mixing, effectively halving the length of the potential core of the jet. The decline in centerline Mach number is not as large as in the axisymmetric case of Fig. 7, probably because of the partial coverage of the jet by the coflow. These experiments prove that mixing enhancement is not specific to axisymmetric jets and also occurs in rectangular and possibly other configurations.

D. Aeroacoustic Resonance

Convergent-divergent nozzles operated at off-design conditions often exhibit resonant tones associated with the presence of shocks *inside* the nozzle (this is different from the phenomenon of screech which is caused by shocks external to the nozzle). This resonance was studied extensively by Zaman & Dahl [26], who conjectured that it is caused by a feedback loop internal to the nozzle and is driven by unsteady laminar boundary layer separation near the throat. For an ideally-expanded Mach number around 1.0, and in a large variety of convergent-divergent nozzles, Zaman & Dahl found that the fundamental resonance frequency scales as

$$\frac{f_{\text{resonance}} L}{a_0} \approx 0.15$$

where L is the throat-to-exit length and a_0 is the stagnation speed of sound. They further noted that tripping the boundary layer near the sonic point reduces or eliminates the tones. Also, according to their study, a nozzle with fully turbulent boundary layer is not expected to produce resonant tones.

The axisymmetric convergent-divergent annular nozzles used in the UCI experiments typically emitted resonant tones. For each nozzle configuration, the tone magnitude was dependent on the nozzle pressure ratio and the relative axial placement of the coflow and jet nozzles, which determined the area ratio and shape of the annular passage. The tone frequency was in general agreement with the relation proposed by Zaman & Dahl, although higher harmonics were occasionally present. The tones could be removed by tripping the boundary layer near the sonic point using strips of adhesive tape. This was an awkward procedure as the tapes would often detach from the nozzle; furthermore, given the small dimensions of the annular passages, even a 0.3-mm-thick tape could change substantially the location of the sonic point. It was observed nevertheless that removal of the tones did not have a substantial effect on mixing enhancement. It was also noted that, in clean nozzles, there were certain pressure ratios for which tones were not emitted while mixing enhancement was evident. This allowed a cleaner determination of the impact of tones on the jet flow. Figure 22 compares two Mach 1.5 jets using the arrangement of Fig. 2(c), one with coflow at NPR=1.64 and the other with coflow at NPR=1.51. The noise spectra and schlieren images of each case are shown, together with a measurement of the centerline Mach number at $x/D_1 = 8$. The NPR=1.64 case emitted a distinct tone at 8 kHz with amplitude of about 7 dB. This frequency is in good agreement with the prediction of Zaman & Dahl [26]. The NPR=1.51 case emitted no discernible tones. As seen in Fig. 22, the case with the tone produced slightly less mixing enhancement than did the case without the tone. One should not generalize this observation. It simply serves to show that their is no causal relation between aeroacoustic resonance and mixing enhancement. In small, axisymmetric nozzles, the two phenomena often overlap, which can easily mislead someone into drawing a direct link between the two. (In fact, the author initially attributed importance to the tones until experiments at NASA proved that mixing enhancement was unrelated to the tones [1]). Further evidence of the lack of such link is that the rectangular convergent-divergent nozzles never emitted tones at any pressure ratio. This is a little surprising as the coflow Reynolds numbers for the rectangular and axisymmetric cases were not very different. It suggests that aeroacoustic resonance may be sensitive to nozzle shape as well as Reynolds number.

Even though resonance phenomena are typically undesirable in large-scale applications, they could be exploited in small devices - like fuel injectors - to enhance mixing further by triggering the most amplified instability modes of the fluid. In liquid injection, for example, the resonant tones emitted by the gaseous coflow may couple with the liquid shedding frequency [28] to

promote breakup of the jet column.

E. Summary

The experiments describe a strong flow instability that occurs when a convergent-divergent nozzle is subjected to pressure ratios within the range exemplified by Figs. 8 and 11. Visual absence of shocks outside the coflow nozzle, and the internal pressure distributions of Fig. 14, indicate that this pressure range corresponds to the phenomenon of supersonic nozzle flow separation. That a separated-flow nozzle provides mixing enhancement may not be surprising at first (the exit flow is messy after all) until one examines the magnitude and onset of this phenomenon. The reversal of trends seen in Figs. 8 and 11 cannot be explained by separated flow alone; a subsonic separated nozzle would not have produced them. The magnitude of mixing enhancement seen in the jet of Figs. 9 and 12 cannot be attributed to just messy initial conditions. Moreover, the fact that the unstable flow can destabilize an adjacent flow (even with partial coverage of the adjacent flow as seen in the rectangular jets), points to a vigorous, dynamic instability mechanism. To gain further insight, one needs to examine in detail the phenomenon of supersonic nozzle flow separation.

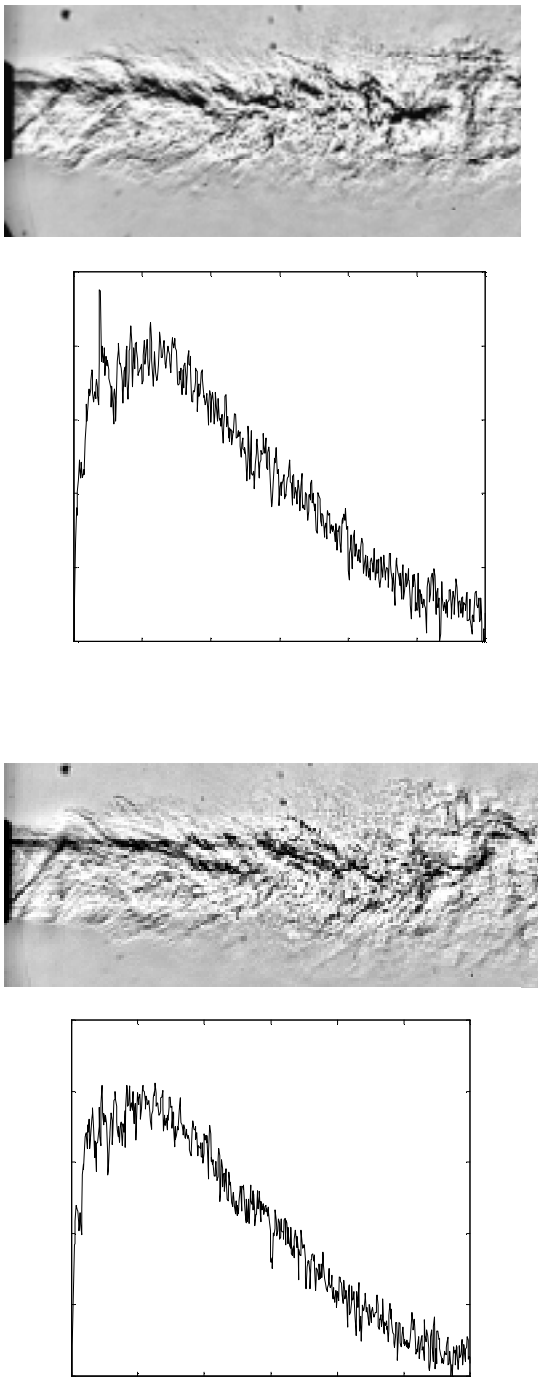

Fig.22 Schlieren images and noise spectra for cases: (a) with resonant tone; (b) without resonant tone. Centerline Mach number at $x/D_1 = 10$ was 1.06 for (a) and 1.03 for (b).

III. Supersonic Nozzle Flow Separation

A. General Observations

The range of coflow pressure ratio for which mixing enhancement occurs (Figs. 8 and 11) and the wall pressure distributions of Fig. 14 hint to a connection between mixing enhancement and supersonic nozzle flow separation. As will be shown below, separation creates a non-uniform pressure field that could be the source of the instability. The fact that mixing enhancement occurred in axisymmetric and rectangular nozzles suggests that nozzle cross sectional shape is not a critical feature of the instability mechanism. In fact, a recent study by Zaman [26], which was partly motivated by the UCI results, showed that even a round convergent-divergent nozzle produces mixing enhancement of the type (although not necessarily of the magnitude) exemplified by Fig. 11. This allows us to focus on the basic phenomenon of separation in a generic convergent-divergent nozzle for obtaining insight into the mechanics of mixing enhancement. Note, however, that nozzle cross section may play a role in amplifying the instability.

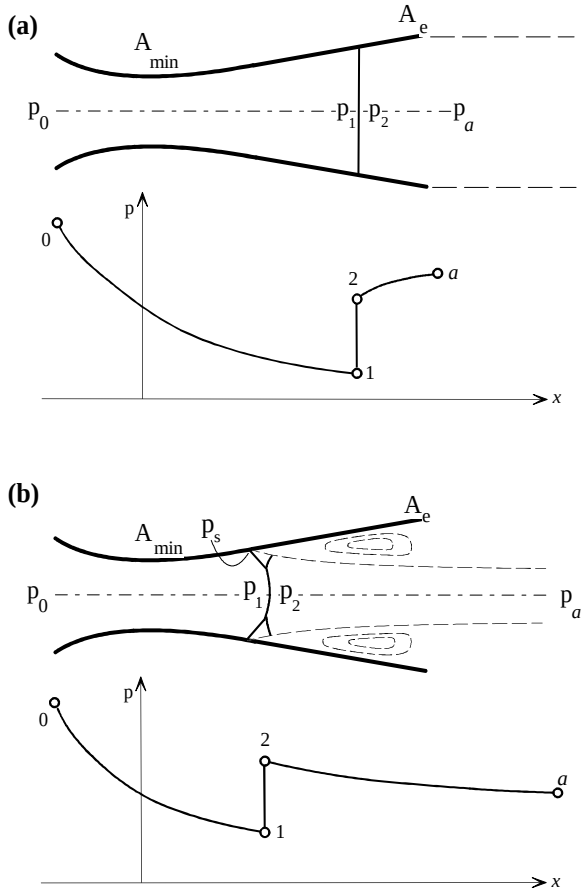

Fig.23 Sketch of shock structure, fluid phenomena, and centerline pressure distributions for overexpanded nozzle. (a) Inviscid case; (b) viscous (separated) case, depicting the underexpansion postulated by Romine [36]. The two cases are compared qualitatively at the same nozzle pressure ratio p_0/p_a.

Supersonic nozzle flow separation occurs in convergent-divergent nozzles subjected to pressure ratios much below their design value, resulting in shock formation inside the nozzle. In the one-dimensional, inviscid treatment of Fig. 23(a), the shock is normal and the emerging flow stays attached to the wall, thus compresses subsonically to the ambient static pressure. In reality flow typically detaches and forms a separation region near the wall, as depicted in Fig. 23(b). For moderate nozzle area ratios a lambda shock is often observed. Flow downstream of the shock is non-uniform with the wall pressure matching the ambient pressure but with a significant overpressure immediately aft of the normal shock. This non-uniformity is a central point of the discussion here.

B. Past Work

There is a large volume of literature dealing with separation in rocket nozzles, which have large expansion ratios. A paramount issue is prediction of separation location, specifically the ratio p_s/p_a (pressure just ahead of separation over ambient pressure). An extensive review of the older literature, and correlation of experimental results in a large variety of nozzles, is given by Morrisette & Goldberg [29]. Their primary conclusion is that zero-pressure-gradient separation predictors, like the method of Reshotko & Tucker [30], give reasonable predictions for nozzles with turbulent separation and large divergence angles. The ratio p_s/p_a is a declining function of the shock Mach number M_s and, as a rule of thumb, is roughly 0.5 for $M_s \approx 2$ and 0.3 for $M_s \approx 4$. Nozzles with laminar separation exhibited higher separation pressure ratios, which shows that the effect of Reynolds number should be included in any comprehensive study of this flow. Separation in nozzles with low local wall angles, such as low-divergence conical nozzles and contoured nozzles, deviated from the above predictions. The close proximity of the wall to the separation shear layer has been cited as a possible reason for the discrepancy.

Computational studies of two-dimensional overexpanded nozzles by Wilmoth & Leavitt [31] and by Hamed & Voyatzis [33, 34] assessed the accuracy of turbulence models for predicting the flow field and thrust performance. The works agree on the basic structure of the separation shock, which consists of the incident shock, Mach stem (normal shock), and separation shock. Thrust predictions were in good agreement with experiments, except at pressure ratios associated with separated flow. A combined experimental and computational work by Hunter [35] offers one of the most comprehensive treatments of this flow. His experimental results on a two-dimensional nozzle with $A_e/A_{\min} = 1.8$ showed two distinct separation regimes: three-dimensional separation with partial reattachment for nozzle pressure ratio NPR$\leq$ 1.8 and fully-detached two-dimensional separation for NPR $\geq$ 2.0. Hunter claims that this transition was not the result of markedly different onset conditions or stronger shock-boundary layer interaction, but instead came about trough the natural tendency of an overexpanded nozzle flow to detach and reach a more efficient thermodynamic balance. As a result, the thrust of the separated case is much higher that that given by inviscid analysis. Notable in Hunter's experiments and simulations was the much higher nozzle pressure ratio required to situate the shock at a given area ratio compared to the inviscid prediction. For example, to place the normal shock just outside the nozzle exit a nozzle pressure ratio NPR=3.4 was required, versus NPR=1.8 predicted in the inviscid case.

Generic methods for boundary-layer separation cannot capture the entirety of events inside a nozzle. Recently, a theoretical model proposed by Romine [36] helps fill

this gap. For shocks with moderate Mach numbers (less than 2.25), Romine postulates that the jet flow emerging from the shock is above ambient pressure and adjusts to the ambient pressure via a gradual underexpansion. The magnitude of the underexpansion is equal to that of the overexpansion, i.e., $p_2/p_a = p_a/p_1$ (see Fig. 23 (b)). It is important to note that this argument applies in the vicinity of the *centerline* of the nozzle, where the shock is normal or close to normal, and not on the walls. On the walls, there is general agreement that flow adjusts to the ambient pressure almost immediately. The underexpanded jet is initially *subsonic* but can eventually reach sonic or low supersonic speeds, thus is a rather unique flow. The higher back pressure felt by the shock pushes the shock upstream of its inviscid location, which explains the much larger NPR (compared to the ideal case) required to position the shock at a given area ratio. The underexpansion is evident in the computational Mach number contours of Hunter [35], although he did not mention it explicitly. Romine's model agrees well with experimental data in rocket nozzles and, as shown below, offers valuable guidance for predicting the occurrence of mixing enhancement. Most importantly it brings to light a region of non-uniform static pressure that could extend past the exit of the nozzle and which could be the key ingredient of the mixing enhancement mechanism.

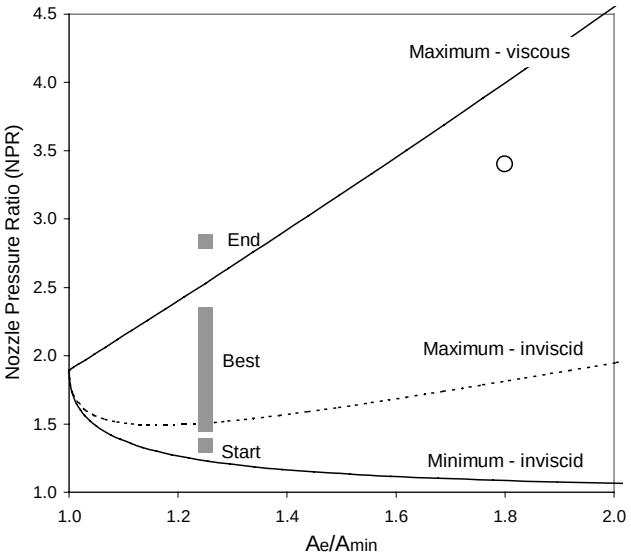

Fig.24 Prediction of NPR versus nozzle area ratio for shock-containing nozzle flow. The theoretical lower limit is based on inviscid, 1D calculation for the onset of sonic flow. The inviscid upper limit is based on 1D flow, while the viscous upper limit is based on the normal-shock separation solution of Romine [36] and is more realistic. Rectangular symbols depict experimental data on the onset, strongest occurrence, and cessation of mixing enhancement in a nozzle with $A_e/A_{\mathsf{min}} = 1.25$. The round symbol denote the pressure ratio for which a normal shock is visualized at the exit of nozzle with $A_e/A_{\mathsf{min}} = 1.80$ [35].

C. Nozzle Pressure Ratio

The range of nozzle pressure ratios for which a shock sits inside a convergent-divergent nozzle is governed by the nozzle area ratio $A_e/A_{\min}$. The lowest NPR corresponds to establishment of sonic flow at the minimum area ($A_{\min} = A_*$), followed by subsonic compression. The inviscid solution involves solving first for the exit Mach number M_e using the subsonic branch of the isentropic area-Mach number relation

$$\frac{A_e}{A_{\min}} = \frac{1}{M_e}\left[\frac{2}{\gamma+1}(1+\frac{\gamma-1}{2}M_e^2)\right]^{\frac{\gamma+1}{2(\gamma-1)}} \qquad (1)$$

and then computing the total-to-static pressure ratio based on M_e

$$\mathrm{NPR}_{\min} = \frac{p_0}{p_a} = \frac{p_0}{p_e} = \left(1+\frac{\gamma-1}{2}M_e^2\right)^{\frac{\gamma}{\gamma-1}} \qquad (2)$$

where p_a is the ambient pressure and p_e is the nozzle exit pressure. The nozzle becomes shock-free when the shock sits at the nozzle exit. The inviscid, one-dimensional prediction is

$$\begin{aligned}\mathrm{NPR}_{\max} &= \frac{p_0}{p_a} = \frac{p_0}{p_2} = \frac{p_0/p_1}{p_2/p_1} \\ &= \frac{\left(1+\frac{\gamma-1}{2}M_1^2\right)^{\frac{\gamma}{\gamma-1}}}{1+\frac{2\gamma}{\gamma+1}(M_1^2-1)} \quad \text{(inviscid)} \qquad (3)\end{aligned}$$

where the numerator is the total-to-static pressure ratio immediately ahead of the shock and the denominator is the static pressure ratio across the shock. The Mach number M_1 is given by the supersonic branch of Eq. 1. As mentioned above, the inviscid theory seriously underestimates the NPR needed to position the shock at a given area ratio. Romine's model [36] offers a simple way to account for the effects of separation. If $p_2/p_a = p_a/p_1$, as Romine proposes, then $p_a/p_1 = \sqrt{p_2/p_1}$, hence

$$\begin{aligned}\mathrm{NPR}_{\max} &= \frac{p_0}{p_a} = \frac{p_0/p_1}{\sqrt{p_2/p_1}} \\ &= \frac{\left(1+\frac{\gamma-1}{2}M_1^2\right)^{\frac{\gamma}{\gamma-1}}}{\sqrt{1+\frac{2\gamma}{\gamma+1}(M_1^2-1)}} \quad \text{(viscous)} \qquad (4)\end{aligned}$$

with M_1 given again by the supersonic branch of Eq. 1.

Figure 24 plots the three limits of NPR: the inviscid lower limit, the inviscid upper limit, and the viscous upper limit. The striking difference between the latter two is again noted. It can only be explained by a subsonic underexpansion following the shock. Overlaid on the plot are experimental data on mixing enhancement in a nozzle with $A_e/A_{\min} = 1.25$, corresponding

to the graph of Fig. 11. "Start" indicates the NPR at which mixing enhancement is first observed and agrees reasonably well with the inviscid prediction of onset of sonic flow in the nozzle. "Best" indicates the NPR range for strong mixing enhancement. "End" denotes the end of mixing enhancement and is in good agreement with the prediction of shock-free nozzle flow. Also shown is Hunter's [35] result for positioning the shock at the exit of a $A_e/A_{\min} = 1.8$ nozzle.

Figure 24 suggests a strong connection between mixing enhancement and flow separation. There is suspicion that the non-uniform pressure field emerging from the separation could trigger instability. Pressure imbalance alone does not explain instability, however. Supersonic over- and under-expanded jets do not exhibit the type of mixing enhancement discussed here. So, if there is a connection, it must have something to do with the peculiar subsonic underexpansion of this flow. The underexpansion aspect of flow separation has never been the subject of experimental investigation. Moreover, the available pressure data in the literature do not capture the underexpansion because all of them were acquired on the nozzle walls, not on the flow centerline.

D. Thrust Prediction

Thrust loss arises mainly from formation of a shock inside the nozzle and the accompanying drop in total pressure. Assuming uniform flow at the nozzle exit and sonic flow at the throat ($A_* = A_{\min}$), the normalized nozzle thrust is

$$\frac{F}{p_0 A_*} = \frac{A_e}{A_*}\left[\frac{p_e}{p_0}\left(1+\gamma M_e^2\right) - \frac{p_a}{p_0}\right] \qquad (5)$$

where the subscript e refers to the nozzle exit plane and subscript a refers to the ambient values. Since the mass flow rate is proportional to $p_0 A_*$, this formulation is convenient for comparing flows of equal mass flow rate. The ideal thrust is that of a flow of equal mass flow rate as the actual flow that has been expanded to the ambient pressure isentropically. The ideal exit Mach number is

$$M_{e_i} = \sqrt{\frac{2}{\gamma-1}\left[\left(\frac{p_0}{p_a}\right)^{(\gamma-1)/\gamma} - 1\right]}$$

and the corresponding area ratio, $(A_e/A_*)_i$, is given by Eq. 1. The ideal normalized thrust is

$$\frac{F_i}{p_0 A_*} = \left(\frac{A_e}{A_*}\right)_i \frac{p_a}{p_0}\,\gamma M_{e_i}^2 \qquad (6)$$

Using Eq. 5 and assuming one-dimensional, inviscid flow, prediction of thrust is straight-forward. However, this prediction will likely be inaccurate for the flows considered here. There are three problems with predicting analytically the thrust of separated nozzle flow. First, the flow is non-uniform at the exit. Second, the shock location–and even whether the shock is inside the nozzle or not–cannot be determined from one-dimensional inviscid theory; see the discussion of the previous section. Third, the normal part of the shock occupies only a fraction of the nozzle cross-sectional where it sits – the rest is occupied by oblique shocks. Thus, only experiment and computation can make reasonable prediction of nozzle thrust. Unfortunately overexpanded nozzle thrust measurements are extremely scarce in the literature. The author was able to find only two such works, one by Hunter [35] for $A_e/A_{\min} = 1.8$ and the other by Wilmoth & Leavitt [31] for $A_e/A_{\min} = 1.3$. Hunter also includes computational predictions of thrust.

The experimental and computational data are summarized in Fig. 25 which plots the percent thrust loss versus nozzle area ratio for NPR=2.0. Also shown on the figure is the inviscid one dimensional prediction. The reader is cautioned that this prediction is likely to be physically and hence quantitatively inaccurate, particularly for the large area ratios. For NPR=2.0 and for all the area ratios covered in Fig. 24, the inviscid theory predicts shock-free nozzle flow with oblique shocks in the jet plume. There is little doubt that in reality the shock occurs inside the nozzle as verified by the aforementioned experiments and computations. The inviscid curve matches well Wilmoth & Leavitt's datum–which could be coincidental–but overestimates by factor of two the thrust loss of Hunter's nozzle. In the absence of more sophisticated tools, the inviscid theory seems to provide a reasonable "first cut" for predicting thrust loss in low-expansion-ratio nozzles, even though it may not represent the actual flow regime. Referring to the experimental data it should be noted that both nozzles had relatively sudden expansions; smoother contours may have reduced the thrust losses. Hunter argues that better control of separation may lead to losses comparable to his computational predictions. Interpolating linearly between the origin and Wilmoth & Leavitt's $A_e/A_{\min} = 1.3$ thrust measurement in Fig. 25 we infer *preliminary* estimates of thrust loss in some of the cases covered: 1.5 % for the flow of Fig. 5(c), where the coflow contributed 22% of the total thrust; 2.7 % for the flow of Fig. 12(b), where the coflow provided all the thrust; and 2.0% for the flow of Fig. 17(b), where the coflow contributed 69% of the total thrust.

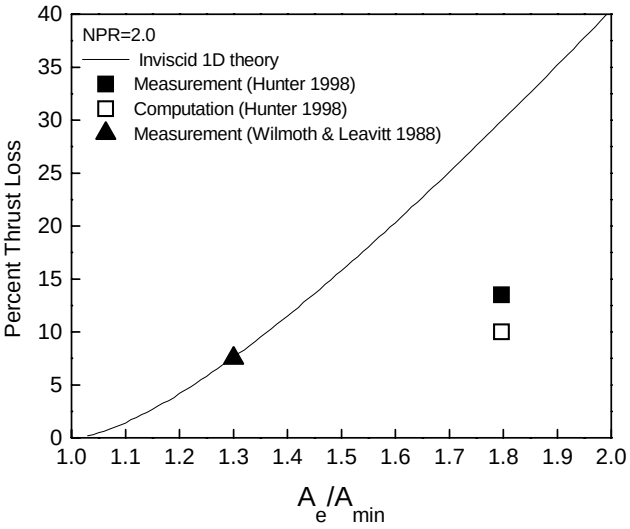

Fig.25 Percent thrust loss versus nozzle area ratio for NPR=2.0. Symbols denote experimental and computational data. Line represents the one-dimensional, inviscid prediction, which is believed to be physically and quantitatively inaccurate.

IV. Future Work

The method of mixing enhancement via secondary parallel injection axial flow is attractive because it involves clean flow paths, simple nozzle shapes, and the potential for small thrust loss. The current understanding of the instability mechanism is admittedly poor, although there is strong evidence that it is linked to the fluid mechanics of supersonic nozzle flow separation. Further insight into the physical mechanisms entails systematic investigation of the basic underlying phenomena. Below are some key elements of such an investigation.

- Prediction of shock location versus nozzle pressure ratio and nozzle area ratio. It is surprising how little is known about this basic flow. Textbooks routinely discuss the one-dimensional, invisid theory. However, as shown earlier, viscosity has a profound effect on this relation. A good model of shock location would help refine the predictions of onset and cessation of mixing enhancement and describe better the loss mechanisms.

- Characterization of the subsonic underexpansion region past the shock. The extent, magnitude, and nature of this region have never been investigated. Is the subsonic underexpansion inherently unstable? Does its magnitude depend on nozzle area ratio as well as nozzle expansion angle?

- Correlation of mixing enhancement with the magnitude and extent of underexpansion. This would confirm or dismiss the hypothesis that the two phenomena are connected.

- Unsteadiness of the internal flow. Even though mixing enhancement is not related to aeroacoustic resonance (for which the internal flow is undoubtedly unsteady), absence of resonant tones does not necessarily mean that the shock structure is perfectly stationary. It is important to investigate possible unsteadiness of the internal flow and correlate it to mixing enhancement.

- Effect of nozzle geometry. So far the discussion has emphasized the effect of the area ratio $A_e/A_{\min}$. Other features of the nozzle shape could also play a vital role. The nozzle expansion angle, for example, affects shock curvature which in turn governs the non-uniformity of the emerging flow.

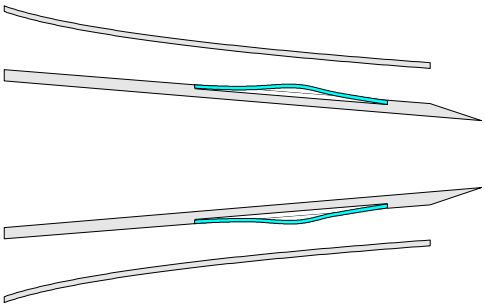

Fig.26 Variable geometry throat for on-demand application of MESPI. Actuation could be pneumatic or mechanical.

Assuming that the subsonic underexpansion is the culprit, an intriguing question is: could the same flow be generated by other means, not involving shocks? This could lead to a virtually loss-free way to enhance mixing. The answer, of course, involves detailed study of the underexpansion as proposed above. Understanding the flow field in an overexpanded nozzle will also pave the way to effective methods for active flow control. Sonic flow is very susceptible to small disturbances, hence is an ideal regime for applying small inputs to achieve large-scale events. One could envision MESPI-type nozzles with small fluidic or mechanical actuators near the throat ($A_{\min}$) that promote further instability by controlling the frequency and the spanwise (2D) or azimuthal (axisymmetric) wavenumber of the disturbances. Application and optimization of *sonic line control* entails in-depth knowledge of the internal flow. In other applications, flexible surfaces would be activated into a convergent-divergent geometry when mixing enhancement is desired and otherwise form a straight channel. This on-demand application would confine thrust losses to the periods mixing enhancement is activated. Figure 26 provides an illustration of such a scheme.

V. Concluding Remarks

Experiments have demonstrated the occurrence of an instability in the plume of convergent-divergent nozzles operated at off-design conditions. There is substantial evidence that this instability occurs when sonic flow is established at the throat of the nozzle and an adverse pressure gradient is generated near the nozzle exit. The instability causes mixing enhancement in the flow itself and can destabilize an adjacent flow. The latter feature enables mixing enhancement of an arbitrary jet via parallel injection of a secondary gas flow. This method of mixing enhancement is characterized by the absence of mechanical mixers, usage of a clean flow path, and good preservation of the axial momentum of the flow. It has the ability to increase substantially the mixing of supersonic jets, which are very stable and in which mechanical mixers inflict substantial penalties. In the supersonic examples presented in this paper, the thrust loss was estimated to be around 1.5%, with potential for even smaller loss with appropriate nozzle design. The underlying physical mechanisms are not well understood although there appears to be a strong connection with the phenomenon of supersonic nozzle flow separation. Specifically, the range of nozzle pressure ratios for which mixing enhancement occurs overlaps with the prediction of separated flow inside the nozzle. Detailed investigation of the internal and external flow phenomena is necessary for understanding and optimizing this method.

Acknowledgments

The phenomenon described in this paper was discovered in the course of research funded by NASA Langley Research Center (Grant NAG-1-1729, monitored by Dr. John M. Seiner). It was subsequently researched under NASA Lewis Grant NAG-3-1981 (Dr. Milo D. Dahl) and NASA Langley Grant NAG-1-2104 (Dr. Thomas D. Norum). The assistance of Ms. Erina Murakami with construction of the rectangular jet apparatus is appreciated.

References

[1] Zaman, K.B.M.Q, and Papamoschou, D., "Study of Mixing Enhancement Observed with a Co-Annular Nozzle Configuration, " AIAA-2000-0094.

[2] Chen, H.-H., and Driscoll, J.F., "Nitric Oxide Levels of Turbulent Jet Diffusion Flames–Effects of Coaxial Air and Other Mixing parameters," 23rd Symposium on Combustion, 1990, pp. 281-288.

[3] Fric, T.F., "Effects of Fuel-Air unmixedness on NOx Emissions, " *Journal of Propulsion Power*, Vol. 9, No. 5, 1993, pp. 708-713.

[4] Schetz, J.A., Hewitt, P.W., and Situ, M., "Tranverse jet breakup and atomization with rapid vaporization along the trajectory," *AIAA Journal*, Vol. 23, No. 4, 1985, pp. 254-261.

[5] Hermanson, J.C., Papas, P., and Kay I.W. "Structure and Penetration of a Supersonic Fluid Jet in Supersonic Flow," *AIAA Journal of Propulsion and Power*, Vol. 10, No.3, pp. 387-393, 1994.

[6] Tillman, T.G., Paterson, R.W., and Presz, W.M., "Supersonic Nozzle Mixer Ejector," *Journal of Propulsion and Power*, Vol.8, No.2, 1992, pp. 513-519.

[7] Sato, H., Mori, M., and Nakamura, T., "Development of a Dry Ultra Low NOx Double Swirler Staged Gas Turbine Combustor," *Journal of Engineering for Gas Turbines and Power*, Vol. 120, No.1, 1998, pp. 41-47.

[8] Harari, R., and Sher, E., "Optimization of a Plain-Jet Airblast Atomizer," *Atomization & Sprays*, Vol. 7, No. 1, 1997, pp. 97-113.

[9] Westley, R., and Lilley, G.M., "An Investigation of the Noise Field from a Small Jet and Methods for Its Reduction," College of Aeronautics, Report 53, Cranfield Univ., England, UK, 1952.

[10] Seiner, J.M. and Gilinski, M.M., "Nozzle Thrust Optimization While Reducing Jet Noise," *AIAA Journal*, Vol. 35, No.3, 1997, pp. 420-427.

[11] Ahuja, K.K. and Brown, W.H., "Shear Flow Control by Mechanical Tabs," AIAA-89-0994.

[12] Zaman, K.B.M.Q., Reeder, M.F., and Samimy, M., "Control of an Axisymmetic Jet Using Vortex Generators," *Physics of Fluids A*, Vol. 6, No.2, 1994, pp. 778-796.

[13] Samimy, M., Kim, J.-H., Clancy, P.S., and Martens, S., "Passive Control of Supersonic Rectangular Jets via Nozzle Trailing-Edge Modifications," *AIAA Journal*, Vol. 36, No.7, 1998, pp. 1230-1239.

[14] Seiner, J.M. and Grosch, C.E., "Mixing Enhancement by Tabs in Round Supersonic Jets," AIAA-98-2326.

[15] Zaman, K.B.M.Q., "Jet Spreading Increase by Passive Control and Associated Performance Penalty," AIAA-99-3505.

[16] Samimy, M., Zaman, K.B.M.Q., and Reeder, M.F., "Effect of Tabs on the Flow and Noise Control of an Axisymmetric Jet," *AIAA Journal*, Vol. 31, 1993, pp. 609-619.

[17] Yu, K.H., and Schadow, K.C., "Cavity-Actuated Supersonic Mixing and Combustion Control," *Combustion and Flame*, Vol. 99, 1994, pp. 295-301.

[18] Kumar, A., Bushnell, D.M., and Hussaini, M.Y., "Mixing Augmentation Technique for Hypervelocity Scramjets," *Journal of Propulsion and Power*, Vol.5, No.5, 1989, pp.514-521.

[19] Dolling, D.S., Fournier, E., and Shau, Y.R., "Effects of Vortex Generators on the Growth of a Compressible Shear layer, *Journal of Propulsion and Power*, Vol.8, No.5, 1992, pp. 1049-1056.

[20] Island, T.C., Urban, W.D., and Mungal, M., "Mixing Enhancement in Compressible Shear Layers via Sub-Boundary layer Disturbances, " *Physics of Fluids*, Vol. 10, No. 4, 1998, pp. 1008-1020.

[21] Strykowksi, P.J., Krothapalli, A., and Jendoubi, S., " The Effect of Counterflow on the Development of Compressible Shear Layers," *Journal of Fluid Mechanics*, Vol. 308, 1996, pp. 63-96.

[22] Van der Veer, M.R., and Strykowski, P.J., "Counterflow Thrust Vector Control of Subsonic Jets: Continuous and Bistable Regimes, " *Journal of Propulsion and Power*, Vol. 13, No. 3, 1997, pp. 412-420.

[23] Raman, G., "Using Controlled Unsteady Fluid Mass Addition to Enhance Jet Mixing," *AIAA Journal*, Vol. 35, No.4, 1997, pp. 647-656.

[24] Weber, Y.S. and Bowers, D.L., "Advancements in Exhaust System Technology for the 21st Century," AIAA-98-3100.

[25] Smith, B.L., and Glezer, A., "Vectoring and Small-Scale Motions Effected in Free Shear Flows Using Synthetic Actuators, " AIAA-97-0213.

[26] Zaman, K.B.M.Q. and Dahl, M.D., "Aeroacoustic Resonance with Convergent-Divergent Nozzles," AIAA-99-0164.

[27] Papamoschou, D. and Debiasi, M. "Noise Measurements in Supersonic Jets Treated with the Mach Wave Elimination Method," *AIAA Journal*, Vol. 37, No.2, 1999, pp. 154-160.

[28] Lasheras, J.C., Villermaux, E., and Hopfinger, E.J., "Break-up and Atomization of a Round Water Jet by a High-Speed Annular Air jet, " *Journal of Fluid Mechanics*, Vol. 357, 1998, pp. 351-379.

[29] Morrisette, E.L., and Goldberg, T.J., "Turbulent Flow Separation Criteria for Overexpanded Supersonic Nozzles," NASA TP 1207, Aug. 1978.

[30] Reshotko, E., and Tucker, M., "Effect of a Discontinuity on Turbulent Boundary Layer Thickness Parameters with Application to Shock-Induced Separation," NACA TN-3454, 1955.

[31] Wilmoth, R.G., and Leavitt, L.D., "Navier Stokes Predictions of Multifunction Nozzle Flows," *Society of Automotive Engineers Transactions*, Vol. 96, Sec.6, Paper 871753, 1987, pp. 6.865-6.879.

[32] Chen, C.L., and Chakravarthy, S.R., "Numerical Investigation of Separated Nozzle Flows," *AIAA Journal*, Vol. 32, No.9, 1994, pp. 1836-1843.

[33] Hamed, A., and Vogiatzis, C., "Overexpanded Two-Dimensional Convergent-Divergent Nozzle Flow Simulations, Assessment of Turbulence Models," *Journal of Propulsion and Power*, Vol. 13, No. 3, 1997, pp. 444-445.

[34] Hamed, A., and Vogiatzis, C., "Overexpanded Two-Dimensional Convergent-Divergent Nozzle Performance, Effects of Three-Dimensional Flow Interactions," *Journal of Propulsion and Power*, Vol. 14, No. 2, 1998, pp. 234-240.

[35] Hunter, C.A., "Experimental, Theoretical and Computational Investigation of Separated Nozzle Flows," AIAA-98-3107.

[36] Romine, G.L., "Nozzle Flow Separation," *AIAA Journal*, Vol. 36, No.9, 1998, pp. 1618-1625.